

REPORT

Strikingly Different Clinicopathological Phenotypes Determined by Progranulin-Mutation Dosage

Katherine R. Smith,^{1,2} John Damiano,³ Silvana Franceschetti,⁴ Stirling Carpenter,⁵ Laura Canafoglia,⁴ Michela Morbin,⁶ Giacomina Rossi,⁶ Davide Pareyson,⁷ Sara E. Mole,⁸ John F. Staropoli,⁹ Katherine B. Sims,⁹ Jada Lewis,¹⁰ Wen-Lang Lin,¹¹ Dennis W. Dickson,¹¹ Hans-Henrik Dahl,³ Melanie Bahlo,^{1,12,*} and Samuel F. Berkovic^{3,*}

We performed hypothesis-free linkage analysis and exome sequencing in a family with two siblings who had neuronal ceroid lipofuscinosis (NCL). Two linkage peaks with maximum LOD scores of 3.07 and 2.97 were found on chromosomes 7 and 17, respectively. Unexpectedly, we found these siblings to be homozygous for a c.813_816del (p.Thr272Serfs*10) mutation in the progranulin gene (*GRN*, granulin precursor) in the latter peak. Heterozygous mutations in *GRN* are a major cause of frontotemporal lobar degeneration with TDP-43 inclusions (FTLD-TDP), the second most common early-onset dementia. Reexamination of progranulin-deficient mice revealed rectilinear profiles typical of NCL. The age-at-onset and neuropathology of FTLD-TDP and NCL are markedly different. Our findings reveal an unanticipated link between a rare and a common neurological disorder and illustrate pleiotropic effects of a mutation in the heterozygous or homozygous states.

The neuronal ceroid lipofuscinoses (NCLs) are neurodegenerative diseases characterized by storage of abnormal lipopigment in lysosomes. The more common childhood-onset forms, which are usually associated with visual failure, are due to recessive mutations in a group of genes believed to be involved in lysosomal processing.¹ Adult-onset cases are rarer and can present with or without retinopathy; the genetic causes are now being unraveled.^{2,3}

We employed genetic linkage analysis and massively parallel sequencing to identify the genetic cause of NCL with retinopathy in a family with apparent recessive inheritance for whom screening of likely known genes (*PPT1* [MIM 600722], *CLN3* [MIM 607042], and *CLN6* [MIM 606725]) was unrewarding. Two siblings with apparently unrelated, healthy parents were affected (Figure 1A). The 28-year-old proband presented with rapidly progressive visual failure at 22 years, followed by major convulsions at 25 years, and myoclonic seizures at 26 years. Clinical examination showed mild cerebellar ataxia, early cognitive deterioration, and retinal dystrophy (Figure 1B). Electroencephalogram (EEG) results showed generalized polyspike wave discharges, electroretinogram results showed severe attenuation of both rod and cone responses, and MRI results showed cerebellar atrophy. Electron microscopic examination of a skin biopsy demonstrated numerous fingerprint profiles in membrane-bound structures in ec-

crine-secretory cells and in endothelium (Figure 1C). The proband's 26-year-old sister began having recurrent convulsions at 23 years, sometimes preceded by visual distortions. Her vision was initially normal but deteriorated when she was 25 years old. Examination revealed cerebellar ataxia and retinal dystrophy. EEG results showed polyspike wave discharges with a posterior emphasis, and MRI results revealed cerebellar atrophy.

Clinical studies were approved by the Human Research Ethics Committee of Austin Health, Melbourne, Australia, and written informed consent was obtained from participating family members. DNA isolated from blood samples of the two affected siblings and their parents was genotyped through the use of Illumina Infinium Human-Hap610W-Quad BeadChip genotyping arrays at the Australian Genome Research Facility (Melbourne). We analyzed genotypes for a subset of 11,572 SNP markers that have high heterozygosity and are in approximate linkage equilibrium (one SNP was chosen per 0.3 cM). Marker selection was performed by the Perl script `linkdatagen.pl`.⁴

Although the parents were not known to be related, they came from nearby small villages in Lombardy, Italy. To determine whether consanguinity was present, we estimated the inbreeding coefficients (*F*) of the affected siblings using FEestim,⁵ obtaining *F* = 0.000 for the affected

¹Bioinformatics Division, The Walter and Eliza Hall Institute of Medical Research, 1G Royal Parade, Parkville, Victoria 3052, Australia; ²Department of Medical Biology, University of Melbourne, Parkville, Victoria 3010, Australia; ³Epilepsy Research Center, Department of Medicine, University of Melbourne, Austin Health, West Heidelberg, Victoria 3081, Australia; ⁴Unit of Neurophysiopathology, Istituto di Ricovero e Cura a Carattere Scientifico (IRCCS) Foundation, Carlo Besta Neurological Institute, 20133 Milan, Italy; ⁵Serviço de Anatomia Patológica, Hospital São João, Porto 4200-319, Portugal; ⁶Division of Neuropathology and Neurology 5, IRCCS Foundation, Carlo Besta Neurological Institute, 20133 Milan, Italy; ⁷Clinic of Central and Peripheral Degenerative Neuropathies Unit, Department of Clinical Neurosciences, IRCCS Foundation, Carlo Besta Neurological Institute, 20133 Milan, Italy; ⁸Medical Research Council Laboratory for Molecular Cell Biology, Molecular Medicine Unit, Institute of Child Health and Department of Genetics, Evolution and Environment, University College London, London WC1E 6BT, UK; ⁹Neurogenetics DNA Diagnostic Laboratory, Massachusetts General Hospital, Center for Human Genetic Research, Boston, MA 02114, USA; ¹⁰Center for Translational Research in Neurodegenerative Disease and Department of Neuroscience, University of Florida, Gainesville, FL 32610, USA; ¹¹Department of Neuroscience, Mayo Clinic, Jacksonville, FL 32224, USA; ¹²Department of Mathematics and Statistics, University of Melbourne, Victoria 3010, Australia

*Correspondence: bahlo@wehi.edu.au (M.B.), s.berkovic@unimelb.edu.au (S.F.B.)

DOI 10.1016/j.ajhg.2012.04.021. ©2012 by The American Society of Human Genetics. All rights reserved.

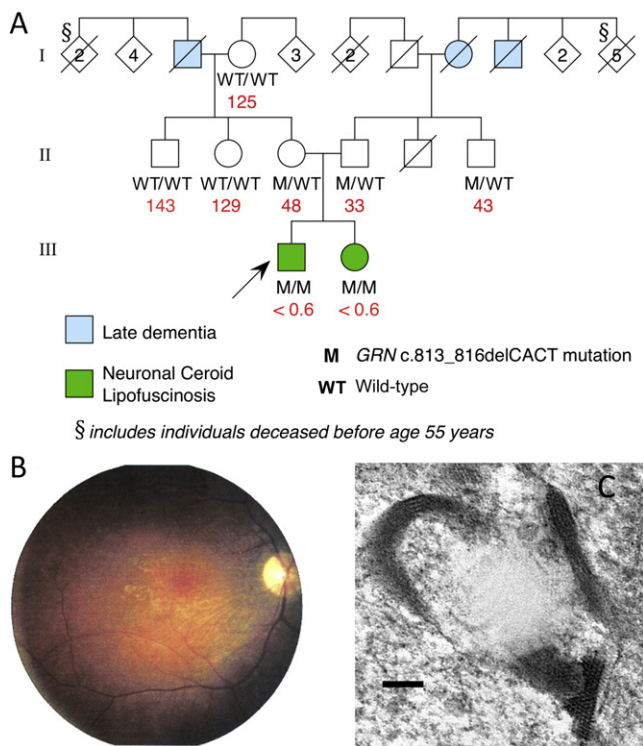


Figure 1. Family Pedigree and Clinical Features of NCL in Proband

(A) Pedigree of family (arrow indicates proband) indicating mutation status for *GRN* (c.813_816del). Plasma progranulin values are shown in red (ng/ml; median normal value is 126 ng/ml).

(B) Retinal photograph of proband showing optic atrophy, arteriolar attenuation, and irregular retinal pigmentation.

(C) Electron micrograph of skin biopsy from the proband. Typical fingerprint profiles within a membrane-bound structure in an eccrine pale cell are shown. The bar indicates 100 nm.

son and $F = 0.006$ for the affected daughter. This suggests that the parents are distantly related (approximately second cousins once removed; expected $F = 0.0078$).

To ascertain the chromosomal locus, we performed an initial multipoint parametric linkage analysis that assumed no relationship between the two parents using MERLIN.⁶ We specified a fully penetrant recessive genetic model, a disease allele frequency of 0.0001, and allele frequencies from the Centre d'Etude du Polymorphisme Humain (CEPH; Utah residents with ancestry from northern and western Europe) HapMap population. FEstim was then used to adjust the LOD scores produced by MERLIN to account for the estimated inbreeding.⁷

This analysis revealed two linkage peaks located on chromosomes 7 and 17 (Figure 2). These peaks do not overlap any of the following genes previously implicated in NCL: *PPT1*, *TPP1*, *CLN3*, *CLN5*, *CLN6*, *MFSD8*, *CLN8*, *CTSD*, or *DNAJC5*. The linkage peak on chromosome 7 achieved a maximum adjusted LOD score of 3.07 and was located between rs1981701 and rs318572 (50.54 to 54.14 cM via deCODE), spanning 3.19 Mb and encompassing 25 genes. The linkage peak on chromosome 17 achieved a maximum adjusted LOD score of 2.97 and was located between

rs2019231 and rs3809854 (70.07 to 73.75 cM); it spanned 5.42 Mb and encompassed 186 genes.

To efficiently identify a potential causative mutation, we sequenced the exomes of the two parents and their affected son. Exome capture and sequencing was performed by Axseq Technologies (Rockville, MD, USA). DNA samples were enriched for approximately 62 Mb of the genome identified as being "exomic" with the use of Illumina TruSeq capture and sequenced using an Illumina HiSeq 2000 machine, generating 110 bp paired-end reads.

Reads were aligned to the hg19 reference genome with the use of Novoalign, with quality score calibration performed. Multimapping reads were removed; potential PCR duplicates were removed with Picard. Variants were called with the mpileup and bcftools view utilities from the SAMtools package^{8,9} and filtered with the vcutils.pl script from the same package. Variants were annotated with ANNOVAR.¹⁰ We used HumVar-trained PolyPhen-2 (v2.1.0r367) to predict the biological impact of nonsynonymous variants.¹¹

Table S1, available online, summarizes the number of reads mapped to each exome, and Table S2 summarizes the distribution of coverage for targeted bases.

We detected 325,946 variants from the reference sequence in at least one member of the trio. No rare (not reported or with frequencies of less than 1% in the 1000 Genomes May 2011 release¹²) exonic or splice-site variants were detected in *PPT1*, *TPP1*, *CLN3*, *CLN5*, *CLN6*, *MFSD8*, *CLN8*, *CTSD*, or *DNAJC5*. A total of 1,688 variants (0.52%) were located within the two linkage regions, of which 352 were rare and 20 were predicted to affect exonic regions or splice sites. All of these 20 variants were located within the linkage peak on chromosome 17. We discarded three variants that resulted in synonymous changes not predicted to affect splicing. Of the remaining 17 variants, three had inferred genotypes following the pattern expected under the consanguineous recessive disease model (i.e., the affected son was homozygous and unaffected parents were heterozygous; missing genotypes were permitted).

The three candidate disease-causing variants are described in Table S3. All three variants were present in dbSNP 132. Two variants (in *DBF4B* [MIM 611661] and *ADAM11* [MIM 155120]) were present in the 1000 Genomes data set, both with an alternate allele frequency of 0.006. The third variant was not present in the 1000 Genomes data set, but was a known pathogenic mutation: a 4 bp deletion in *GRN* (MIM 138945; NM_002087.2), which encodes progranulin (also known as the granulin precursor). The c.813_816del mutation (rs63749877) results in a frameshift and premature termination of translation 10 residues downstream (p.Thr272Serfs*10). Sanger sequencing confirmed that the variant was genuine and segregated as expected in the family, with the mother and father heterozygous for the variant and both affected children homozygous.

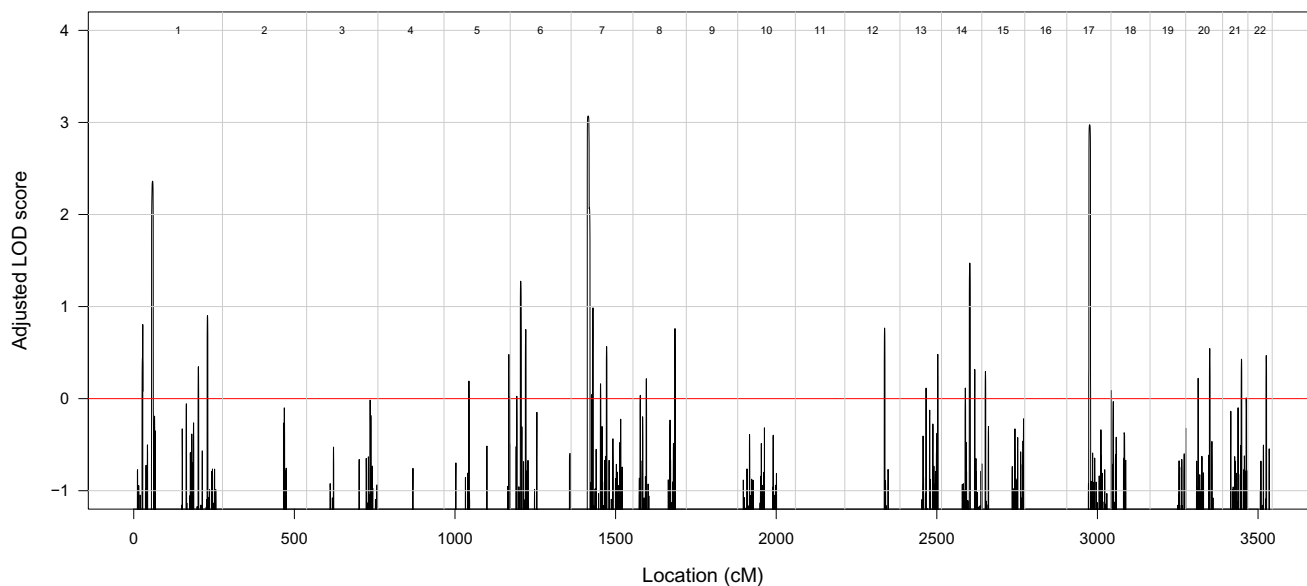


Figure 2. Results of Linkage Analysis

Autosomal genome-wide LOD scores, adjusted for inbreeding, for the family under a fully penetrant recessive genetic model.

Heterozygous c.813_816del *GRN* mutations are known to cause frontotemporal lobar degeneration^{13–16} (FTLD-TDP; MIM 607485). This presents in later life, so we reevaluated the family for features of frontal lobe dementia. There was a history of late dementia (approximately seventh decade) in the maternal grandfather, paternal grandmother, and great uncle; as all three individuals are deceased, pathological diagnoses could not be made, and DNA could not be obtained. A number of older relatives had died before 55 years of age, so a more obvious pattern of autosomal-dominant dementia may have been masked. The parents, both heterozygous for the mutation, were in their fifties and healthy. DNA from all available family members was screened. The results (Figure 1) indicate that the mother must have inherited the c.813_816del mutation from her father, who had dementia, and that an additional family member in the parents' generation is a c.813_816del heterozygote. Plasma progranulin was measured in available family members with a commercial kit (Human Progranulin ELISA Kit, AdipoGen, Seoul, South Korea).¹⁷ Plasma progranulin correlated with the genotypes; values were 125–143 ng/ml in three individuals with no copies of the deletion (median normal value: 126 ng/ml¹⁷), 33–48 ng/ml in the three heterozygous subjects, which is below the cutoff value (62 ng/ml) for predicting heterozygous null mutations,¹⁷ and undetectable (<0.6 ng/ml) in the two homozygous affected siblings (Figure 1A).

Subsequently, we sequenced 20 unrelated cases of proven or suspected adult NCL wherein known NCL genes had been excluded. All 13 exons, exon-intron boundaries, and untranslated regions of *GRN* were PCR-amplified, sequenced with the BigDye Terminator v3.1 Cycle Sequencing protocol, and run on an ABI 3730XL DNA

Analyzer (Life Technologies, Carlsbad, CA, USA). We did not find homozygous or compound-heterozygous mutations in any of these individuals, although one was found to be heterozygous for the most common *GRN* mutation, c.1477C>T (p.Arg493*; rs63751294).¹⁸ This patient presented with limb dystonia, spasticity, gait disturbance, apraxia, and dementia at the age of 46. Death occurred around the age of 48–49. We excluded the possibility that this individual had a partial deletion of the second *GRN* allele by performing a multiplex ligation-dependent probe amplification assay. We were unable to reevaluate the original diagnosis of NCL as the original electron micrographs and tissue samples were unavailable. This diagnosis was made on the basis of lymphocyte inclusions, which may be unreliable in adult NCL; we suspect that the individual may have had FTLD-TDP misdiagnosed as adult NCL. We also sequenced the same regions of *GRN* for 188 anonymous blood-bank controls without detecting any known mutations or novel variants.

Ahmed et al. previously generated mice deficient in the orthologous *Gm* (*Gm*^{-/-}) and reported accumulation of abnormal intraneuronal ubiquitin-positive autofluorescent lipofuscin detected by light microscopy.¹⁹ This finding has since been replicated with the use of independently generated *Gm*-deficient mice.²⁰ Electron microscopic examination of fixed brain tissue from the Ahmed et al. mice revealed abundant rectilinear profiles diagnostic of NCL (Figure 3). Animal studies were performed in accordance with the Mayo Clinic Institutional Animal Care and Use Committee.

We report that homozygous c.813_816del mutations in *GRN* cause adult-onset NCL and suggest that this locus be designated CLN11. This result is remarkable, given that mutations in this gene are an important cause of

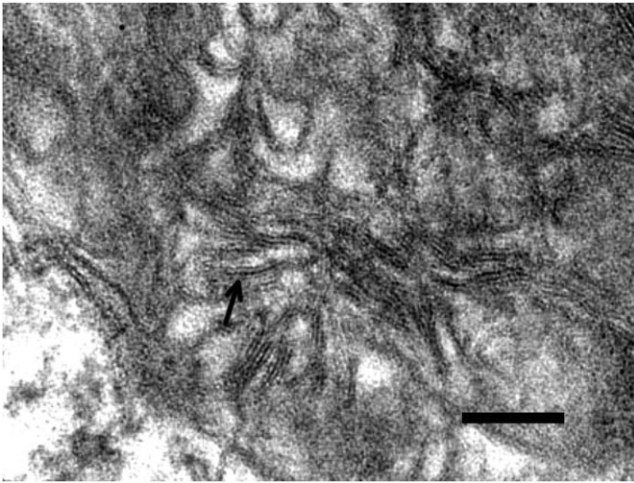


Figure 3. NCL Pathology in Progranulin-Deficient Mice

Electron micrograph showing a high-power view of one of the storage granules in a neuron from the habenula of a *Gm*^{-/-} mouse. The pattern corresponds to the rectilinear complex, which, along with fingerprint profiles, is characteristic of most types of NCL. The arrow points to a pentalaminar profile. The bar indicates 100 nm.

FTLD-TDP in the heterozygous state and that the two clinically distinct neurological disorders have very different pathologies.

Clinically, mutations in specific genes usually determine important phenotypes in either the heterozygous or homozygous state, but not both. In classical recessive disorders, heterozygous individuals are usually healthy, asymptomatic carriers, although there may be a clinically trivial or biochemical phenotype or sometimes even a survival advantage, such as for sickle cell trait (MIM 603903).²¹ In classical dominant disorders, the population allele frequency is low, so homozygous individuals are exceptional, except in inbred communities.²² When observed, such rare homozygous cases may differ little from heterozygous family members (e.g., in Huntington disease [MIM 143100] and epidermolysis bullosa simplex [MIM 131900]) or have a more severe form of the same phenotype, suggesting an additive effect on the gene product dysfunction (e.g., in Marfan syndrome [MIM 154700], achondroplasia [MIM 100800], and Charcot-Marie-Tooth disease [MIM 118200]).²²

One example of different diseases with homozygous versus heterozygous mutations involves the gene that encodes acid beta-glucosidase (*GBA* [MIM 606463]). Homozygous *GBA* mutations have been long known to cause the various forms of Gaucher disease (MIMs 608013, 230800, 230900, 231000, and 231005), where there is storage of glucocerebroside. More recently, various heterozygous *GBA* mutations have been shown to increase the risk of late-onset Parkinson disease (MIM 168600), not as a Mendelian trait but rather as a susceptibility factor.^{23,24}

Although the present result was unexpected and we did not identify additional cases, the finding of similar and

diagnostic electron-microscopic features of NCL in the human material and in the progranulin-deficient mouse supports our conclusion of strikingly different phenotypes for this *GRN* mutation depending on whether it is homozygous or heterozygous. The sibling pair had early-adult onset of severe retinal disease with seizures, ataxia, and cognitive change. Although brain biopsies were not available from the siblings, the mouse brain pathology mirrored the known human pathology of NCL in its storage of abnormal autofluorescent lipopigment with characteristic ultrastructural features in neurons.^{25,26} This contrasts with FTLD-TDP due to heterozygous *GRN* mutation; the disorder presents in later life with behavioral and cognitive impairment, but seizures are unusual, and ataxia and retinal involvement are absent. The pathology does not reveal lipopigment storage material but rather neurons with TDP-43-immunoreactive neuronal and glial inclusions.^{27,28}

To the best of our knowledge, homozygous mutations have not previously been reported in *GRN*. Indeed, Bruni et al.²⁹ found no homozygotes in a highly consanguineous Calabrian family in which 19 individuals were found to be heterozygous for a c.1144dup (p.Thr382Asnfs*32) mutation in *GRN*. The authors speculated that the loss of both *GRN* alleles might cause embryonic lethality,²⁹ but our data showing homozygotes with undetectable progranulin levels and the viability of the *Gm*^{-/-} mouse show that progranulin deficiency is compatible with life.

Progranulin has multiple physiological roles, and it influences inflammation, early embryogenesis, tumorigenesis, and adult tissue repair.³⁰ How haploinsufficiency causes FTLD-TDP remains uncertain. In *Caenorhabditis elegans*, progranulin deficiency causes more rapid clearance of apoptotic cells and inadvertently results in the clearance of neurons that would otherwise recover from initiation of apoptosis.³¹ This observation, however, does not explain how progranulin deficiency would result in NCL. Given the link between NCL and proteins that affect lysosomal processing, the association between *GRN* mutation and NCL suggests that progranulin has a lysosomal function. There is good evidence that progranulin is neurotrophic or neuroprotective,³⁰ potentially through the modulation of survival signaling. Disruption of cell signaling processes could conceivably result in rapid “aging” of unprotected progranulin-deficient cells with respect to lipofuscinosis. Indeed, homozygous *GRN* deficiency in mice results in microglial activation, increased ubiquitination, and excess lipopigment deposition.¹⁹

The history of dementia in this family was not regarded as remarkable when first assessed. Early death in many older family members masked the likely autosomal-dominant pattern on both sides of the family (Figure 1A). It has been estimated that 50% of c.813_816del heterozygotes show symptoms by the age of 63 and that 97.3% are symptomatic by the age of 73.¹⁴ Thus, the discovery of homozygous mutation in children presents an unexpected ethical dilemma in terms of new knowledge

regarding the likelihood of late-life dementia in the parents and other healthy heterozygotes.

With the recent widespread implementation of massively parallel sequencing to uncover causes of hitherto obscure early-onset recessive phenotypes,³² even in single families as here, further examples of pleiotropic effects of homozygous and heterozygous mutations may emerge. This will create opportunities for better pathophysiological understanding, but may also result in unexpected ethical quandaries upon the emergence of age-dependent heterozygous phenotypes.

Supplemental Data

Supplemental Data include three tables and can be found with this article online at <http://www.cell.com/AJHG/>.

Acknowledgments

K.R.S. is supported by a PhD scholarship funded by the Pratt Foundation. S.E.B. is supported by a National Health and Medical Research Council (NHMRC) Australia Fellowship and an NHMRC Program Grant. M.B. is supported by an Australian Research Council (ARC) Future Fellowship and an NHMRC Program Grant. S.E.M. is supported by the Medical Research Council. The Batten Disease Support and Research Association supported S.E.M., J.S., and K.S. We thank Pawan Mann and Olivia Galante for technical assistance; Danya Vears, Robyn Ferguson, and Karen Oliver for technical support; the Rare NCL Gene Consortium for encouraging collaborative research on variant NCL cases; and the families and physicians for providing samples.

Received: February 16, 2012

Revised: March 21, 2012

Accepted: April 26, 2012

Published online: May 17, 2012

Web Resources

The URLs for data presented herein are as follows:

Online Mendelian Inheritance in Man (OMIM), <http://www.omim.org/>

Novoalign, www.novocraft.com

Picard, <http://picard.sourceforge.net/>

References

1. Mole, S.E., and Williams, R.E. (2010). Neuronal Ceroid-Lipofuscinoses. In *GeneReviews*, R.A. Pagon, T.D. Bird, and C.R. Dolan, et al., eds. (Seattle, WA: University of Washington), <http://www.ncbi.nlm.nih.gov/books/NBK1428/>.
2. Arsov, T., Smith, K.R., Damiano, J., Franceschetti, S., Canafoglia, L., Bromhead, C.J., Andermann, E., Vears, D.F., Cossette, P., Rajagopalan, S., et al. (2011). Kufs disease, the major adult form of neuronal ceroid lipofuscinosis, caused by mutations in CLN6. *Am. J. Hum. Genet.* 88, 566–573.
3. Nosková, L., Stránecký, V., Hartmannová, H., Přistoupilová, A., Barešová, V., Ivánek, R., Hůlková, H., Jahnová, H., van der Zee, J., Staropoli, J.F., et al. (2011). Mutations in DNAJC5, encoding cysteine-string protein alpha, cause autosomal-dominant adult-onset neuronal ceroid lipofuscinosis. *Am. J. Hum. Genet.* 89, 241–252.
4. Bahlo, M., and Bromhead, C.J. (2009). Generating linkage mapping files from Affymetrix SNP chip data. *Bioinformatics* 25, 1961–1962.
5. Leutenegger, A.L., Prum, B., Génin, E., Verny, C., Lemainque, A., Clerget-Darpoux, F., and Thompson, E.A. (2003). Estimation of the inbreeding coefficient through use of genomic data. *Am. J. Hum. Genet.* 73, 516–523.
6. Abecasis, G.R., Cherny, S.S., Cookson, W.O., and Cardon, L.R. (2002). Merlin—rapid analysis of dense genetic maps using sparse gene flow trees. *Nat. Genet.* 30, 97–101.
7. Leutenegger, A.L., Labalme, A., Genin, E., Toutain, A., Steichen, E., Clerget-Darpoux, F., and Edery, P. (2006). Using genomic inbreeding coefficient estimates for homozygosity mapping of rare recessive traits: application to Taybi-Linder syndrome. *Am. J. Hum. Genet.* 79, 62–66.
8. Li, H. (2011). A statistical framework for SNP calling, mutation discovery, association mapping and population genetical parameter estimation from sequencing data. *Bioinformatics* 27, 2987–2993.
9. Li, H., Ruan, J., and Durbin, R. (2008). Mapping short DNA sequencing reads and calling variants using mapping quality scores. *Genome Res.* 18, 1851–1858.
10. Wang, K., Li, M., and Hakonarson, H. (2010). ANNOVAR: functional annotation of genetic variants from high-throughput sequencing data. *Nucleic Acids Res.* 38, e164.
11. Adzhubei, I.A., Schmidt, S., Peshkin, L., Ramensky, V.E., Gerasimova, A., Bork, P., Kondrashov, A.S., and Sunyaev, S.R. (2010). A method and server for predicting damaging missense mutations. *Nat. Methods* 7, 248–249.
12. Durbin, R.M., Abecasis, G.R., Altshuler, D.L., Auton, A., Brooks, L.D., Gibbs, R.A., Hurles, M.E., and McVean, G.A.; 1000 Genomes Project Consortium. (2010). A map of human genome variation from population-scale sequencing. *Nature* 467, 1061–1073.
13. Benussi, L., Binetti, G., Sina, E., Gigola, L., Bettecken, T., Meitinger, T., and Ghidoni, R. (2008). A novel deletion in progranulin gene is associated with FTDP-17 and CBS. *Neurobiol. Aging* 29, 427–435.
14. Benussi, L., Ghidoni, R., Pegoiani, E., Moretti, D.V., Zanetti, O., and Binetti, G. (2009). Progranulin Leu271LeufsX10 is one of the most common FTL and CBS associated mutations worldwide. *Neurobiol. Dis.* 33, 379–385.
15. Le Ber, I., Camuzat, A., Hannequin, D., Pasquier, F., Guedj, E., Rovelet-Lecrux, A., Hahn-Barma, V., van der Zee, J., Clot, F., Bakchine, S., et al; French research network on FTD/FTD-MND. (2008). Phenotype variability in progranulin mutation carriers: a clinical, neuropsychological, imaging and genetic study. *Brain* 131, 732–746.
16. Yu, C.-E., Bird, T.D., Bekris, L.M., Montine, T.J., Leverenz, J.B., Steinbart, E., Galloway, N.M., Feldman, H., Woltjer, R., Miller, C.A., et al. (2010). The spectrum of mutations in progranulin: a collaborative study screening 545 cases of neurodegeneration. *Arch. Neurol.* 67, 161–170.
17. Ghidoni, R., Stoppani, E., Rossi, G., Piccoli, E., Albertini, V., Paterlini, A., Glionna, M., Pegoiani, E., Agnati, L.F., Fenoglio, C., et al. (2012). Optimal plasma progranulin cutoff value for predicting null progranulin mutations in neurodegenerative diseases: a multicenter Italian study. *Neurodegener. Dis.* 9, 121–127.

18. Rademakers, R., Baker, M., Gass, J., Adamson, J., Huey, E.D., Momeni, P., Spina, S., Coppola, G., Karydas, A.M., Stewart, H., et al. (2007). Phenotypic variability associated with progranulin haploinsufficiency in patients with the common 1477C→T (Arg493X) mutation: an international initiative. *Lancet Neurol.* *6*, 857–868.
19. Ahmed, Z., Sheng, H., Xu, Y.F., Lin, W.-L., Innes, A.E., Gass, J., Yu, X., Wuertzer, C.A., Hou, H., Chiba, S., et al. (2010). Accelerated lipofuscinosis and ubiquitination in granulin knockout mice suggest a role for progranulin in successful aging. *Am. J. Pathol.* *177*, 311–324.
20. Petkau, T.L., Neal, S.J., Milnerwood, A., Mew, A., Hill, A.M., Orban, P., Gregg, J., Lu, G., Feldman, H.H., Mackenzie, I.R.A., et al. (2012). Synaptic dysfunction in progranulin-deficient mice. *Neurobiol. Dis.* *45*, 711–722.
21. Pasvol, G., Weatherall, D.J., and Wilson, R.J.M. (1978). Cellular mechanism for the protective effect of haemoglobin S against *P. falciparum* malaria. *Nature* *274*, 701–703.
22. Zlotogora, J. (1997). Dominance and homozygosity. *Am. J. Med. Genet.* *68*, 412–416.
23. Goker-Alpan, O., Giasson, B.I., Eblan, M.J., Nguyen, J., Hurtig, H.I., Lee, V.M.-Y., Trojanowski, J.Q., and Sidransky, E. (2006). Glucocerebrosidase mutations are an important risk factor for Lewy body disorders. *Neurology* *67*, 908–910.
24. Goker-Alpan, O., Schiffmann, R., LaMarca, M.E., Nussbaum, R.L., McInerney-Leo, A., and Sidransky, E. (2004). Parkinsonism among Gaucher disease carriers. *J. Med. Genet.* *41*, 937–940.
25. Anderson, G., Elleder, M., and Goebel, H.H. (2011). Morphological diagnostic and pathological considerations. In *The neuronal ceroid lipofuscinoses (Batten disease)*, S.E. Mole, R.E. Williams, and H.H. Goebel, eds. (Oxford, UK: Oxford University Press), pp. 35–49.
26. Carpenter, S., Karpati, G., Andermann, F., Jacob, J.C., and Andermann, E. (1977). The ultrastructural characteristics of the abnormal cytosomes in Batten-Kufs' disease. *Brain* *100*, 137–156.
27. Josephs, K.A., Ahmed, Z., Katsuse, O., Parisi, J.F., Boeve, B.F., Knopman, D.S., Petersen, R.C., Davies, P., Duara, R., Graff-Radford, N.R., et al. (2007). Neuropathologic features of frontotemporal lobar degeneration with ubiquitin-positive inclusions with progranulin gene (PGRN) mutations. *J. Neuropathol. Exp. Neurol.* *66*, 142–151.
28. Mackenzie, I.R.A., Baker, M., Pickering-Brown, S., Hsiung, G.-Y.R., Lindholm, C., Dwosh, E., Gass, J., Cannon, A., Rademakers, R., Hutton, M., and Feldman, H.H. (2006). The neuropathology of frontotemporal lobar degeneration caused by mutations in the progranulin gene. *Brain* *129*, 3081–3090.
29. Bruni, A.C., Momeni, P., Bernardi, L., Tomaino, C., Frangi-pane, F., Elder, J., Kawarai, T., Sato, C., Pradella, S., Wakutani, Y., et al. (2007). Heterogeneity within a large kindred with frontotemporal dementia: a novel progranulin mutation. *Neurology* *69*, 140–147.
30. Bateman, A., and Bennett, H.P.J. (2009). The granulin gene family: from cancer to dementia. *Bioessays* *31*, 1245–1254.
31. Kao, A.W., Eisenhut, R.J., Martens, L.H., Nakamura, A., Huang, A., Bagley, J.A., Zhou, P., de Luis, A., Neukomm, L.J., Cabello, J., et al. (2011). A neurodegenerative disease mutation that accelerates the clearance of apoptotic cells. *Proc. Natl. Acad. Sci. USA* *108*, 4441–4446.
32. Najmabadi, H., Hu, H., Garshasbi, M., Zemojtel, T., Abedini, S.S., Chen, W., Hosseini, M., Behjati, F., Haas, S., Jamali, P., et al. (2011). Deep sequencing reveals 50 novel genes for recessive cognitive disorders. *Nature* *478*, 57–63.